

HOSTED BY



Contents lists available at ScienceDirect

Journal of King Saud University – Science

journal homepage: www.sciencedirect.com

Original article

Biogenic AgNPs Synthesized using *Nyctanthes arbor-tristis* L. fruit for antimicrobial & dye degradation efficiencies

Lakshika Sharma^a, Mamta Dhiman^a, Abhishek Dadhich^a, Madan Mohan Sharma^{a,*}, Prashant Kaushik^b^a Department of Biosciences, Manipal University Jaipur, Dehmi Kalan, Near JVK Toll Plaza, Jaipur-Ajmer Expressway, Jaipur 303007, Rajasthan, India^b Instituto de Conservación y Mejora de la Agrodiversidad Valenciana, Universitat Politècnica de València, Valencia, Spain

ARTICLE INFO

Article history:

Received 23 July 2022

Revised 23 January 2023

Accepted 16 February 2023

Available online 3 March 2023

Keywords:

Green synthesis

Silver nanoparticles

Nyctanthes arbor-tristis L.

Antimicrobial assessment

Catalytic efficiencies

ABSTRACT

Enduring demand of sustainable environment encourages the novel green approach of fruit waste utilization to synthesize silver nanoparticles. Herein, aqueous extract of *Nyctanthes arbor-tristis* (NAT) fruit, was used as reducing agent to formulate silver nanoparticles (AgNPs), synthesized silver NPs were observed spectrophotometrically at 460 nm reflecting sharp peak. The average crystalline size of the X-ray diffraction was assessed to be 29.39 nm. Reduction in the FTIR peaks revealed substantial role of phytoconstituents (alcohol, polyphenol, amides etc.) in single step method to produce AgNPs. About 20–60 nm, spherical shaped NPs were observed under TEM (Transmission electron microscopy) and SEM (Scanning electron microscopy). Moreover, the EDX (Energy-dispersive X-ray spectroscopy) evaluation revealed the distinct peak of Ag with 27.5% weight. Negative value i.e. –31.5 mv of zeta potential confirmed virtuous stability & dispersion of produced NPs. Nyc. *Nyctanthes* based AgNPs exhibited efficient catalytic activity in NaBH₄ mediated reduction of mordant orange- 1 (MO-1) and methylene blue (MB). The results showed that Nyc.-AgNPs degraded more than 80% to both dyes. In addition, Nyc.-AgNPs unveiled significant antimicrobial role against different bacterial & fungal strains. The attained outcomes proposed that the NAT mediated AgNPs would be an efficient source to approach various environmental and biomedical applications.

© 2023 The Author(s). Published by Elsevier B.V. on behalf of King Saud University. This is an open access article under the CC BY-NC-ND license (<http://creativecommons.org/licenses/by-nc-nd/4.0/>).

1. Introduction

Green nanotechnology is observing as congregating proficiency of the current scenario owing to its excellent structural stability overages and its diversified potentiality towards the major areas of science (Abdulsahib, 2021; David and Moldovan, 2020). Amongst the different metal nanoparticles (MNPs), silver nanoparticles (AgNPs) are considered as one of the important NPs, because of its inimitable assets including good conductivity, antifungal, antiviral, antibacterial, chemical stability, cytotoxic activities, waste water treatment and targeted drug delivery (Gul et al., 2021; Haggag et al., 2019; Jain et al., 2021; Jebri et al., 2020). For example chitosan entrapped *Aegle marmelos* silver NPs were

reported to treat cervical cancer, it showed dose dependent cytotoxic effect against HeLa cell lines through the inhibition of β actin, N-cadherin, SNAIL and increasing the levels of E-cadherin, caspase3 & 9 (Sukumar et al., 2022). Different physical and chemical routes have been used to synthesise the silver NPs, allied with certain limitations like high cost, use of hazardous and toxic chemicals etc.. Consequently, there is an instantaneous necessity to evolve an alternative method based on green approach, which is non-hazardous, eco-friendly, worthwhile and possess several human therapeutic applications (e.g. in wound healing, arthritic disease, etc.). Currently, plant mediated synthesis of silver NPs has been widely considered due to its eco-friendly approach as well as effective reduction efficiencies. Formerly, different plants such as *Sterculia urens*, *Tinospora cordifolia*, *Conocarpus Lancifolius*, *Glochidion candolleianum*, *Tragopogon collinus* etc. being used to synthesize AgNPs (Balachandar et al., 2022; Dhiman et al., 2021; Mittal et al., 2017; Moodley et al., 2018; Oves et al., 2022; Seifpour et al., 2020). Besides, *Nyctanthes* fruits have been also reported to possess different type of bioactive compounds, which can be used as an efficient reducing agent to synthesize the metal nanoparticles. Different type of dye effluents accumulated in water bodies can directly or indirectly affects the human population by causing

* Corresponding author.

E-mail address: madanmohan.sharma@jaipur.manipal.edu (M.M. Sharma).

Peer review under responsibility of King Saud University.



Production and hosting by Elsevier

<https://doi.org/10.1016/j.jksus.2023.102614>

1018-3647/© 2023 The Author(s). Published by Elsevier B.V. on behalf of King Saud University.

This is an open access article under the CC BY-NC-ND license (<http://creativecommons.org/licenses/by-nc-nd/4.0/>).

various incurable disease. Methylene blue (cationic thiazine dye) and Mordant orange- 1 (azo dye) is also included in list of water pollutants which is widely utilized in the textile industry as an important colouring source (Fito et al., 2020). To overwhelm the obstacles associated with the traditionally used degradation methods, nanoparticle derived catalytic degradation is currently accessible by the researchers to upsurge the catalytic experiments for the deduction of some harmful organic pollutants (Pandey et al., 2020). Besides, Antibiotic resistance reduces the effectiveness of treating infections and diseases in animals, humans, as well as plants. Henceforth, the uses of NPs have emerged as novel tools that can be effectively used to combat deadly bacterial infections. The limitations of conventional antimicrobials, such as antibiotic resistance, can be overcome via nanoparticle-based techniques (Gupta et al., 2019). Therefore, the present research laid emphasis on utilization of phyto waste material (*Nyctanthes* fruit) as a chief source of silver reducing & capping agent to fabricate AgNPs, characterization and their cytotoxic evaluation on selected fungal & bacterial species and also assessed efficient environmental applications in catalytic degradation of hazardous MB & MO-1 dyes.

2. Materials and methods

2.1. Materials

Silver nitrate (99.0% pure) NaBH_4 , & MB, MO-1 were procured from Sigma Aldrich, India. Analytical grade deionized water were used to prepared all type of aqueous solutions.

2.2. Assortment & preliminary processing of *Nyctanthes arbor-tristis* fruits

Dried fallen fruits of *N. arbor-tristis*, (during February-March) were collected from plant established in Vatika infotech City, Theekaraya (Jaipur), and thoroughly rinsed with tap water followed by Milli-Q to eradicate dust particles. 5.0 g of crushed fruits were added into 100 ml of Milli-Q water and kept on hotplate for 10 min boiling. Afterwards; Whatman Grade 1 filter paper was used to collect the clear filtrate.

2.3. Phytosynthesis of AgNPs

AgNPs were synthesized by reducing AgNO_3 solution at a range of 1–5 mM in the occurrence of the NAT fruit extract (1–5%). A volume of 40 ml of fruit extract was mixed with 60 ml of AgNO_3 (2 mM) solution and kept at normal room temperature for 24 hr. Afterwards, there is no changes was found in the reaction mixture, to overwhelm this difficulty the same reaction mixture was kept into the orbital shaker at 35 °C & 180 rpm for 24 hrs. For the assessment of optimization studies different parameters were carried out such as variation in the ratios of aqueous plant extract & AgNO_3 solution, temperature (25° to 55°C), variable time (6–30hr), pH (3–11), all the experimental steps were performed in dark condition.

2.4. Purification of nanoparticles

Synthesized Nyc.-AgNPs were collected in purified form via performing centrifugation at 10,000 rpm (5 min) after resultant pellet washed thrice with deionized water to take off unreduced Ag (I) ions & extra fruit extracted metabolites.

2.5. Characterization

Uv-visible spectroscopy (Shimadzu UV2600) were used to record UV-vis spectra with 1 nm resolution and wavelength range between 350 and 750 nm. Fourier transform infrared (FTIR, Bruker alpha) spectroscopy was performed to recognize bioactive compounds (functional group) present in aqueous fruit extract, contributed their effectual role in the capping, reduction as well as stabilization of Ag ions, measured in the frequency range of 500 to 4000 cm^{-1} based on the Attenuated total reflection (ATR) method. While the surface morphology, shape & size of Nyc.-AgNPs were revealed using SEM Jeol (USA) & TEM. The crystallographic nature of the Nyc.-AgNPs was examined using X-ray powder diffraction. The long lasting stability of silver NPs was measured through zeta potential technique (ZEN 5600), which designates the alteration in surface charge with respect to time.

2.6. Antimicrobial sensitivity testing

The microorganisms considered for antimicrobial susceptibility assessment were: *E. coli* (*Escherichia coli*), *P. syringae* (*Pseudomonas syringae*), *S. aureus* (*Staphylococcus aureus*), *P. fragi* (*Pseudomonas fragi*), *S. putrefaciens* (*Shewanella putrefaciens*), *S. epidermidis* (*Staphylococcus epidermidis*) and *A. flavus* (*Aspergillus flavus*). Minimum inhibitory zone (MIC) was calculated using well diffusion method. All tests were executed in triplicate and average results were calculated.

2.7. Assessment of bacterial cell membrane damage

The structural modifications in the cell surface morphology of *E. coli* and *S. aureus* were examined using FESEM. The properly growth conditioned bacterial suspensions was mixed with Nyc.-AgNPs and incubated for 24 hr. at 37 °C with shaking conditions. Further, 2 ml of control (without treated with AgNPs) as well as 2 ml of treated bacterial suspensions were subjected for centrifugation at 5000 rpm for 5 min at 4 °C. Resultant, pellet were washed thrice with distilled water & spread on glass slide via adding Milli Q water and subjected for SEM analysis.

2.8. Catalytic degradation measurements

Nyctanthes based silver nanoparticles were used as nanocatalyst to study NaBH_4 mediated degradation of MB (methylene blue) and MO-1 (mordant orange 1). The experiment was done in a standard UV quartz cell cuvette. Formerly, 2 ml (100 μM) of methylene blue and MO-1 was mixed with 0.5 ml (0.01 M) of NaBH_4 (aqueous) & 0.5 ml of Synthesized Ag nanoparticles. The degradation efficiency of AgNPs against the studied dyes were observed using Shimadzu UV2600 spectrophotometer. The MB and MO-1 absorbance were measured in test solutions at 664 nm and 385 nm respectively.

The given formulas were used to calculate the degradation efficiency (%) & reaction rate constant (pseudo-first order) in test & control with relevant time interval:

$$\text{Degradation efficiency}(\%) = (A_0 - A_t/A_0) \times 100 \quad (1)$$

$$\text{Pseudo - first - order}(-kt) = \ln(A_t/A_0) \quad (2)$$

where A_0 - Initial absorbance of dye.

A_t - Absorbance obtained after each time interval.

K- Degradation reaction rate constant.

3. Result and discussion

3.1. Biosynthesis and UV-vis spectral profiling of synthesized Nyc.-AgNPs

3.1.1. Visual inspection

Addition of NAT fruit extract induces conversion in colour from orange to dark brown, which endorsed the biological reduction of silver ions into AgNPs as well as considered as a preliminary authentication of AgNPs fabrication (Fig. 1) (Al-Rajhi et al., 2022; Dhiman et al., 2021; Samanta et al., 2022).

3.1.2. UV-Vis spectroscopy

UV spectra profiling/ λ_{max} value of reaction mixture recorded between 350 and 750 nm. Though, a sharp peak was logged at 460 nm with 0.5% plant extract and 2 mM AgNO₃ solution. Similarly, previous findings also concluded the same SPR peak between the ranges of 450–500 nm, considered as a reference peak apropos for AgNPs formation (Ali et al., 2016; Kredy, 2018).

3.1.2.1. Influence of time on the formation of AgNPs. UV-visible spectrum was recorded with the interval of 6 hr. Initially up to 6 hr. the colour of the reaction mixture and absorbance between reference wavelength ranges 450 to 500 were not observed. Further, as the time passes till 24 hr. with incessant shaking conditions, colour of the reaction mixture changes with 460 nm λ_{max} value, recorded via UV-visible spectra (Fig. 2a). Upto 24 hr. UV-Vis spectra showed

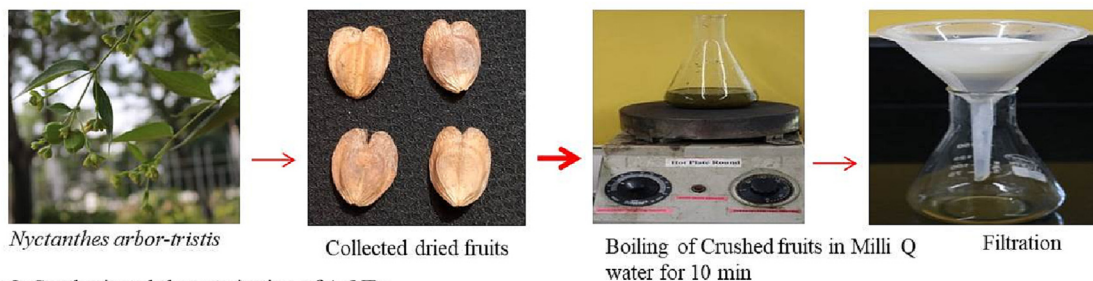
good peak reference to AgNPs synthesis. Further, with the increased time duration overlapped spectra were found (Fig. 2a).

3.1.2.2. Effect of reactant concentration. Amongst the tested concentrations of AgNO₃ and plant extract, optimum results were obtained with the 0.5% fruit extract and 2 mM AgNO₃, showed clear peak at 460 nm (Khane et al., 2022; Kumar et al., 2017) (Fig. 2b). Afterwards, obtained results were used for further experimental analysis.

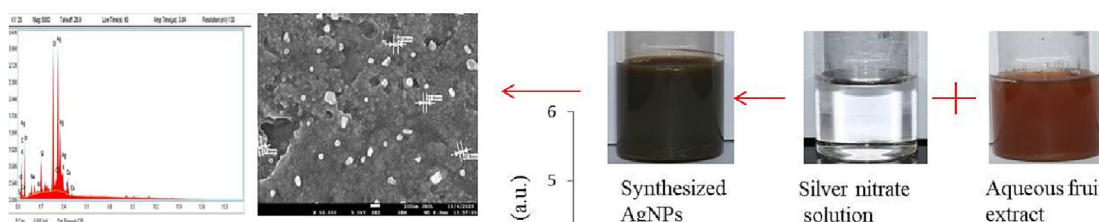
3.1.2.3. Impact of temperature on the fabrication of AgNPs. Fig. 2c revealed the UV-visible spectra of Nyc.-AgNPs at different temperature ranges 25 to 55 °C with the increased in temperature, reduction of Ag ions was also enhanced, indicating through rapid colour change of the solution. Optimum temperature was recorded 55 °C. Obtained results were completely correlated with some previous finding (Gou et al., 2015; Tyavambiza et al., 2021; Verma and Mehata, 2016). Beyond 55 °C decreased peak was found.

3.1.2.4. Effect of pH. No sharp peak was observed with the acidic solution, while with the increased pH towards alkaline conditions, absorbance was also increased. Although, a clear and sharp peak was observed with alkaline pH, it was clearly shown in (Fig. 2d). Henceforth, pH 11 was found to be an optimized pH for Nyc.-AgNPs formation. This result on alkaline pH is supported by (Kedi et al., 2018; Verma and Mehata, 2016).

Step 1: Sample preparation



Step 2: Synthesis and characterization of AgNPs



Step 3: Biological application of synthesized AgNPs

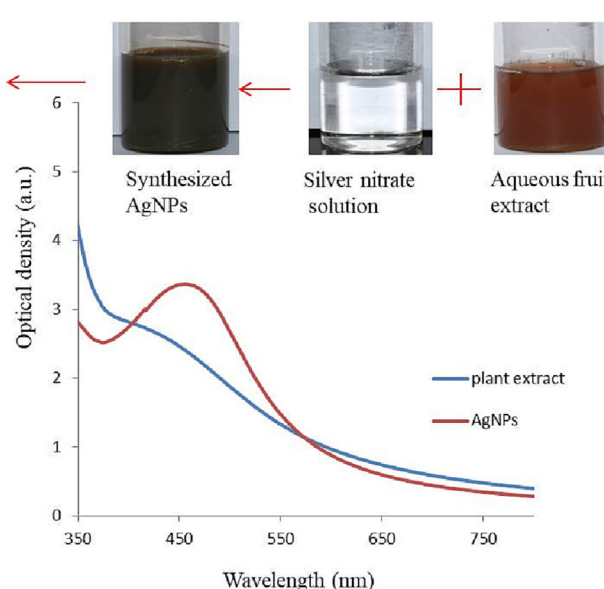
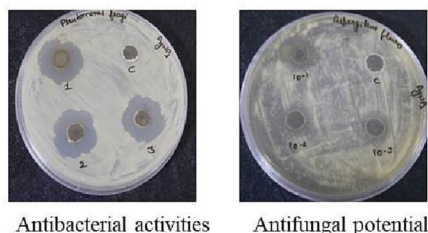


Fig. 1. Schematic illustration of biogenic synthesis of AgNPs using *Nyctanthes arbor-tristis* fruit extract & its antimicrobial efficiencies.

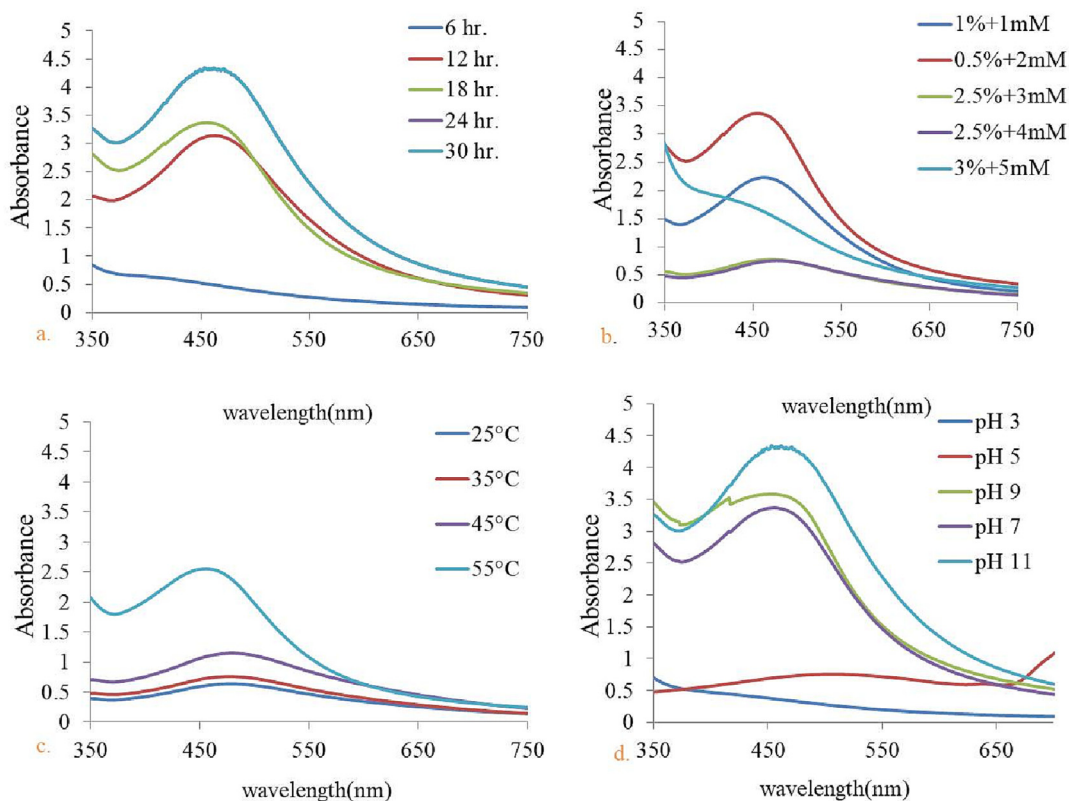


Fig. 2. UV-Vis spectrum of Nyc.-AgNPs obtained for (a) different reaction time (6–30 hr.) & (b) with different concentration of AgNO₃ and plant extract after 12 hr. of incubation, (c) with increasing range of temperature (25 °C–55 °C) (d) various pH values (3–11).

3.2. Infrared spectral analysis

Comparative phytochemical profile of aqueous fruit extract and synthesized Nyc.-AgNPs showed transmission peaks with reduced band intensities at 3845, 3743, 3617, 3096, 2352, 1742, 1649, 1525, 1008, 873, 629, 524 cm⁻¹ (Fig. 3). The obtained peaks at 3845, 3617, 3096 cm⁻¹ (between the series of 4000–3000 cm⁻¹)

consisted for O–H stretching (hydroxyl functional group), also deliberated for the incidence of polyphenols with primary & secondary amine group of proteins (Cheng et al., 2014; Coates, 2006; Hamouda et al., 2019). Vibrational stretching around 2352, 1649, 1525 cm⁻¹ wavelength showed involvement of C–O, (–C=C–) or N–O respectively. The FTIR band around 1008 cm⁻¹ was assigned to (C–O) (Tripathi et al., 2017). Despite, 873, 629,

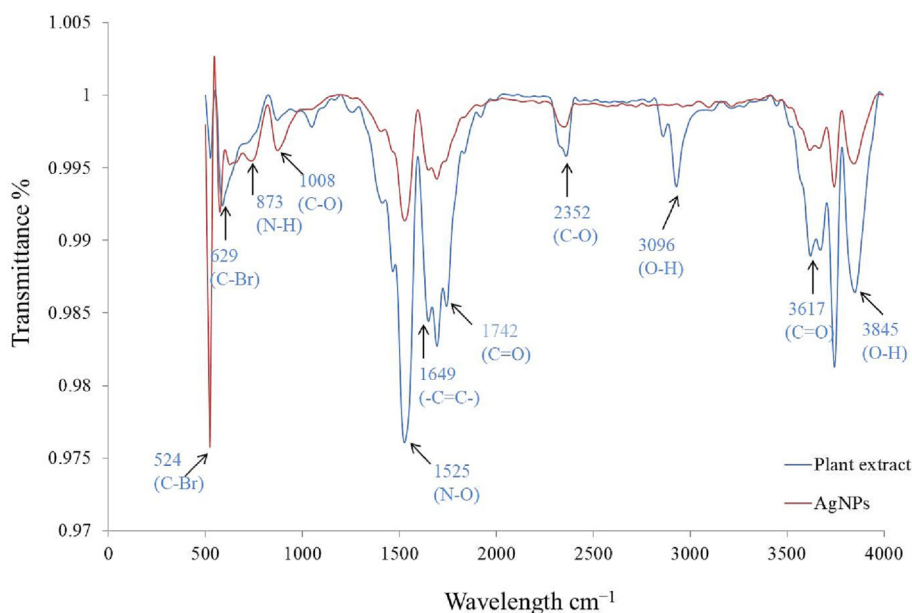


Fig. 3. FTIR spectrums of fruit extract & synthesized Nyc.-AgNPs.

524 cm^{-1} peaks were perceived ranges between 1000 and 500 cm^{-1} , revealing existence of C–Br, C–H, O–H groups respectively (alkyl halide). The interpretation of FTIR data revealed substantial role of phytoconstituents (alcohol, polyphenol, amides etc.) in single step technique to yield AgNPs by averting cluster development and providing steadiness in the medium.

3.3. Scanning electron microscopy

SEM examination endorses the spherical shape of AgNPs with the approx 20–60 nm particle size (Fig. 4a). These outcomes were sturdily reinforced by some published studies (Ghotekar et al., 2019; Jusoh et al., 2019; Kumar et al., 2019). Energy-dispersive X-ray spectroscopy (EDX), describe the elemental constituents of produced materials. Nyc. The SEM-EDX analysis of synthesized AgNPs confirms the presence of Ag ions (27.5%) and some other elements such as, carbon, oxygen, and chlorine act as reducing & capping agents (Fig. 4b,c).

3.4. Zeta potential distribution

Intensive negative value of zeta potential, considered as an evidence about the efficiency of capping agent's for the stabilization of the nanoparticles (Ashour et al., 2015; Bogireddy et al., 2016; Sharifi-Rad et al., 2021). Zeta potential analysis of Nyc. based AgNPs determined the negative value i.e. -31.5 mv & confirmed virtuous stability and dispersion of produced NPs. (Fig. 4d) This electric $-ve$ charge, induces resilient repulsive force between the particles, averts from accumulation (Varadavenkatesan et al., 2019).

3.5. X-ray diffraction (XRD)

Fig. 5a illustrated the X-ray Diffraction pattern of the green synthesized AgNPs. The diffraction peaks at 38.10° , 44.33° , 64.42° , and 77.29° are analogous to (1 1 1), (200), (220), and (3 1 1) reflection planes respectively, accredited to face centered cubic structure of silver nanocrystals. Other resultant peaks relevant to the organic compound, present in the extract (Thiruvengadam and Bansod, 2020) (library ref code 96-901-3047, Suh,I.-K., Ohta, H., Wased, Y., Journal of Materials Sciences, 23, 757-760, (1988).

Using the XRD spectrum, the average size (crystallite) of MNPs was calculated via Debye–Scherer Equation (Holzwarth and Gibson, 2011):

$$D = 0.95\lambda/\beta\cos\theta \quad (3)$$

where, D = average crystallite size, β is line broadening in radians, θ is the Bragg's angle & λ = X-ray wavelength. The calculated average crystallite size of the AgNPs around 29.39 nm (Table 1). Analogous outcomes were also concluded in some previous findings (Atalar et al., 2021; Faisal et al., 2020).

3.6. TGA – Analysis

Thermal gravimetric analysis (TGA) provides information about purity & thermal stability of synthesized silver NPs. It is clearly reflected from Fig. 5b the initial weight loss between the temperatures range 0°C – 100°C is observed owed to the water eradication from the organic environment of the NPs, substantiates that the plant based AgNPs are an excellent materials for absorbing moisture in various fields of applications (Traiwatcharanon et al.,

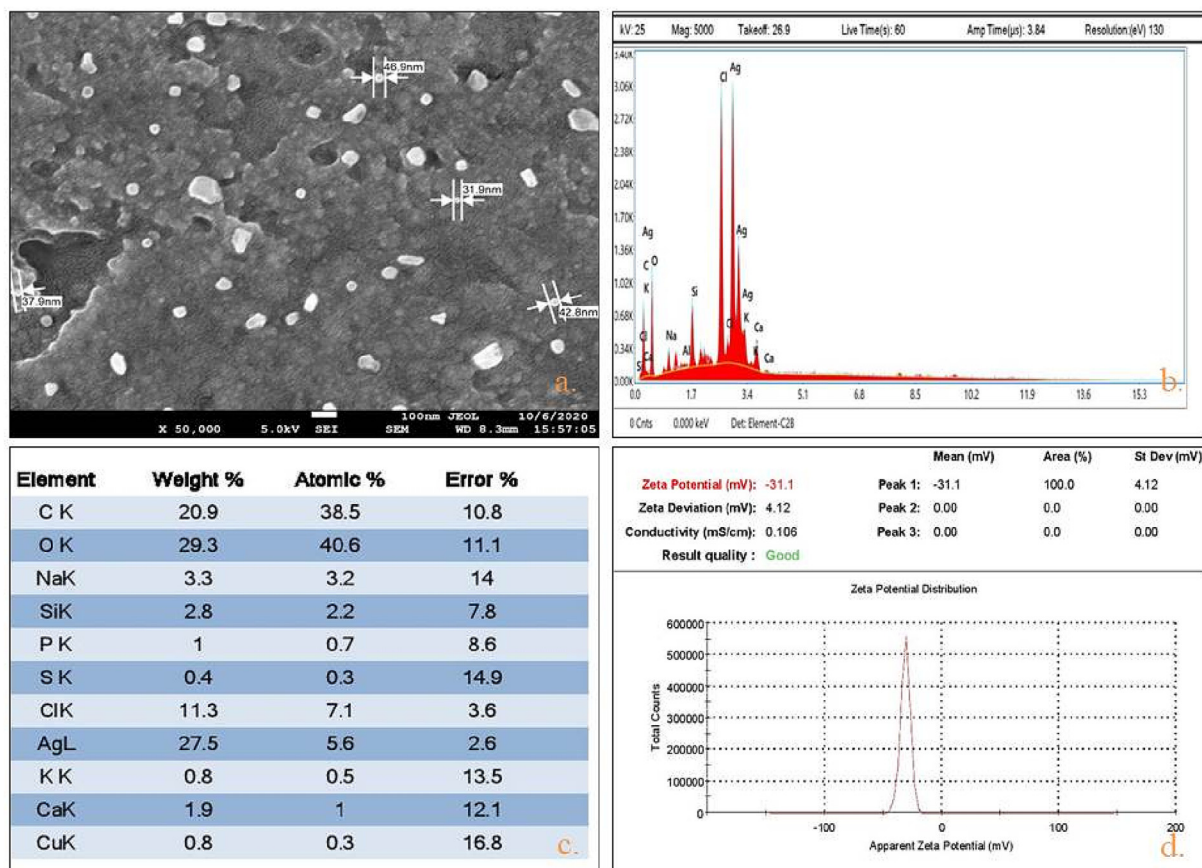


Fig. 4. Characterization of Synthesized Nyc.-AgNPs using (a) SEM analysis (size range (20–60 nm), (b,c) EDX spectroscopy (Ag 27.5 %), and (d) zeta potential stability valuation (-31.1 mv).

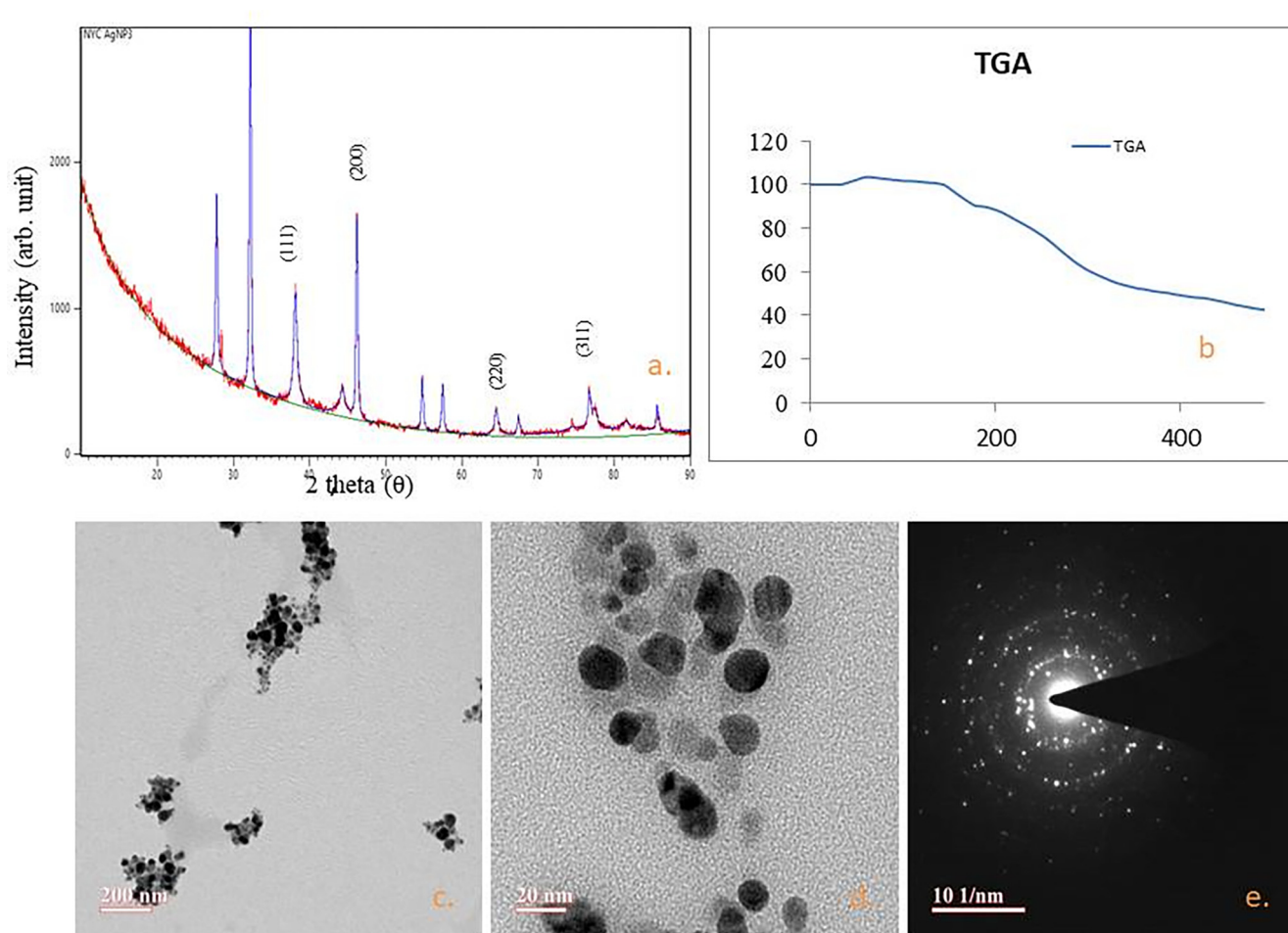


Fig. 5. (a) XRD pattern of bio synthesized AgNPs. Vertical lines relate to face centered cubic (fcc) crystal structure of silver, (b) TGA graph of biosynthesized NPs, (c-e) Transmission electron microscopy images of silver nanoparticles.

Table 1
Particle size calculation of *Nyctanthes* mediated AgNPs.

S.no.	2θ of the intense peak (deg)	d-spacing [Å]	FWHM of intense peak (β) radians	Size of the particle (D) nm
1	38.1023	111	0.4998	17.57
2	44.3395	200	1.0083	8.89
3	64.4234	220	0.3199	30.67
4	77.2944	311	0.1759	60.43
The average value of the crystalline size of nanoparticles of silver				29.39

2017). The mass loss at 200–300 °C was occurred due to the cellulosic materials. The deprivation pattern of phytoconstituents was lasting until 490 °C. Similar consequences have been studied by other researchers (Ali et al., 2015).

3.7. High-resolution transmission electron microscopy (HRTEM) analysis

Fig. 5(c-e) revealed the presence of spherical Ag NPs. Some previous results are available in the support of the current observation relates to polydispersed nature of silver NPs with 20–50 nm size, ensured through TEM (Mittal et al., 2020; Ojha et al., 2017).

3.8. Antimicrobial assessment

According to the results, aqueous extract which is used as a control did not show any kind of antimicrobial activity, while *Nyc.*-AgNPs showed dose dependent antimicrobial potential against studied bacterial as well as fungal strains. Results have been pre-

sented in the form of zone of inhibition (ZOI in millimeters), in Table 2. *Nyc.*-AgNPs showed significant antibacterial effect against *P. fragi* i.e. 24.9 ± 0.10 mm. Besides, the ZOI reached 27.75 ± 0.25 mm for *E. coli*, 15.5 ± 0.50 mm for *P. syringae*, and 18.2 ± 0.46 mm for *S. aureus* (Fig. 6). The lower inhibition zones/MIC was observed between 0.15 mg/ml to 0.002 mg/ml for biogenic AgNPs. The MIC of Synthesized AgNPs was obtained at 0.15 mg/ml against, *P. fragi* and *P. syringae* respectively. Despite, antifungal activity was tested against *A. flavus*, found significant inhibition zone i.e. 18.1 ± 0.15 mm with 10 mg/ml concentration and MIC was found at 0.15 mg/ml of Synthesized AgNPs (Fig. 7). Similar results were concluded with some other findings (Adnan et al., 2022; Castillo-Henríquez et al., 2020; de Jesús Ruíz-Baltazar et al., 2017; Guerra et al., 2020).

3.9. SEM morphological study

SEM analysis of treated bacteria was done to elucidate the morphological changes occurred during the *Nyc.*-AgNPs treat-

Table 2
Inhibitory Effect of Nyc.-AgNPs against different microbial strains.

Nyc.-AgNPs conc. (mg/ml)	Zone of inhibition against bacterial & fungal pathogens (mm)						
	<i>S. aureus</i>	<i>P. fragi</i>	<i>P. syringae</i>	<i>S. putrefaciens</i>	<i>S. epidermidis</i>	<i>E. coli</i>	<i>A. flavus</i>
10	18.2 ± 0.46	24.9 ± 0.10	15.5 ± 0.50	22.5 ± 0.11	20.0 ± 0.00	27.75 ± 0.25	18.00 ± 0.15
5	17.5 ± 0.50	22.0 ± 1.00	14.75 ± 0.25	19.5 ± 0.50	20.6 ± 0.57	27.00 ± 0.00	16.16 ± 0.28
2.5	17.0 ± 0.00	19.25 ± 0.25	14.1 ± 0.10	18.6 ± 0.57	19.25 ± 0.25	21.3 ± 0.57	15.33 ± 0.57
1.25	15.75 ± 0.30	16.25 ± 0.25	12.75 ± 0.25	18.0 ± 0.00	18.45 ± 0.45	19.1 ± 0.15	14.13 ± 0.15
0.62	13.5 ± 0.20	15.5 ± 0.50	13 ± 0.00	16.75 ± 0.25	15.5 ± 0.50	18.2 ± 0.26	13.20 ± 0.26
0.31	12.5 ± 0.51	14.2 ± 0.34	12.45 ± 0.45	16.50 ± 0.57	13.25 ± 0.25	17.5 ± 0.50	11.50 ± 0.50
0.15	10.0 ± 0.75	11 ± 0.00	11.8 ± 0.76	15.52 ± 0.28	10.25 ± 0.25	16.25 ± 0.57	10.66 ± 0.57
0.07	-	-	-	12.50 ± 1.15	-	12.50 ± 0.50	-
0.03	-	-	-	-	-	-	-
0.01	-	-	-	-	-	-	-
0.005	-	-	-	-	-	-	-
0.002	-	-	-	-	-	-	-

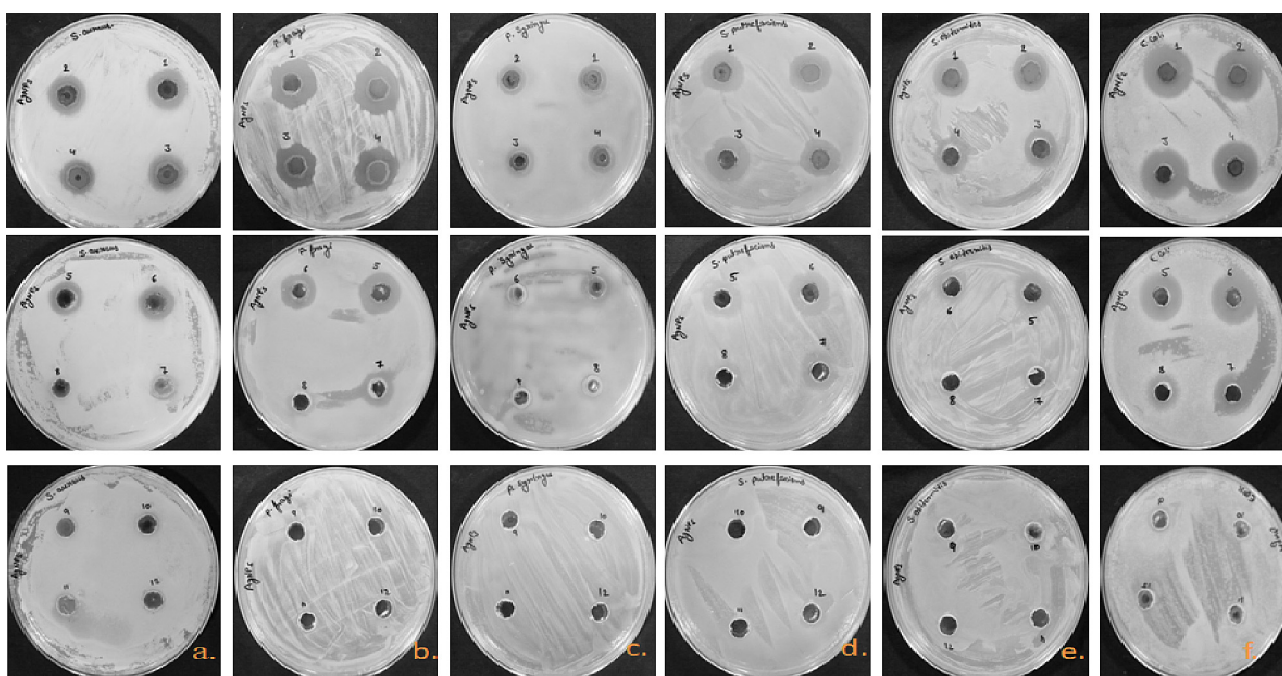


Fig. 6. Antimicrobial susceptibility well diffusion method. ZOI of Nyc-AgNPs at different concentrations (1–12; 10, 5, 2.5, 1.25, 0.62, 0.31, 0.15, 0.07, 0.03, 0.01, 0.005, 0.002 mg/ml). (a), (b), (c), (d), (e) against pathogenic strains *S. aureus*, *P. fragi*, *P. syringae*, *S. putrefaciens*, *S. epidermidis*, *E. coli*.

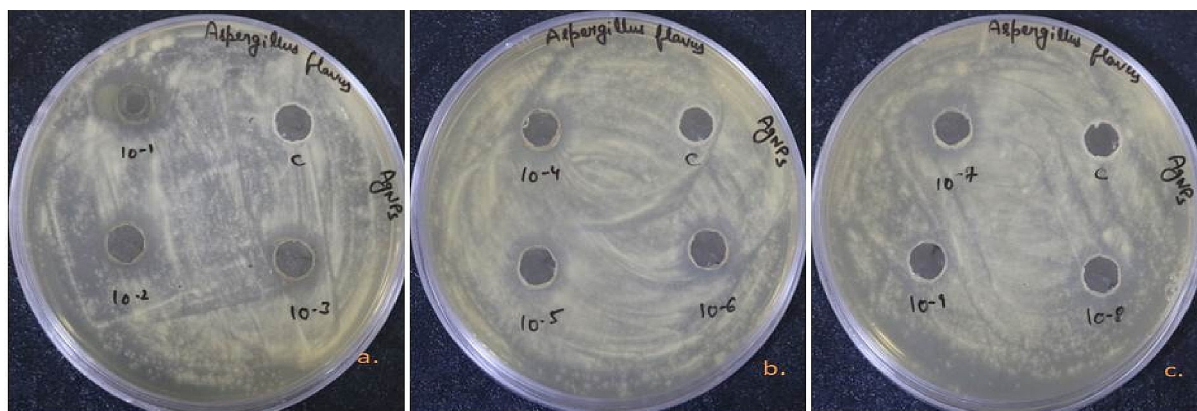


Fig. 7. Antifungal efficiency of Nyc.-AgNPs (a-c) at different concentrations (10^{-1} – 10^{-9} ; 10 mg/ml, 5 mg/ml, 2.5 mg/ml, 1.25 mg/ml, 0.62 mg/ml, 0.31 mg/ml, 0.15 mg/ml, 0.07 mg/ml, 0.03 mg/ml & C; aqueous fruit extract) against *A. flavus*.

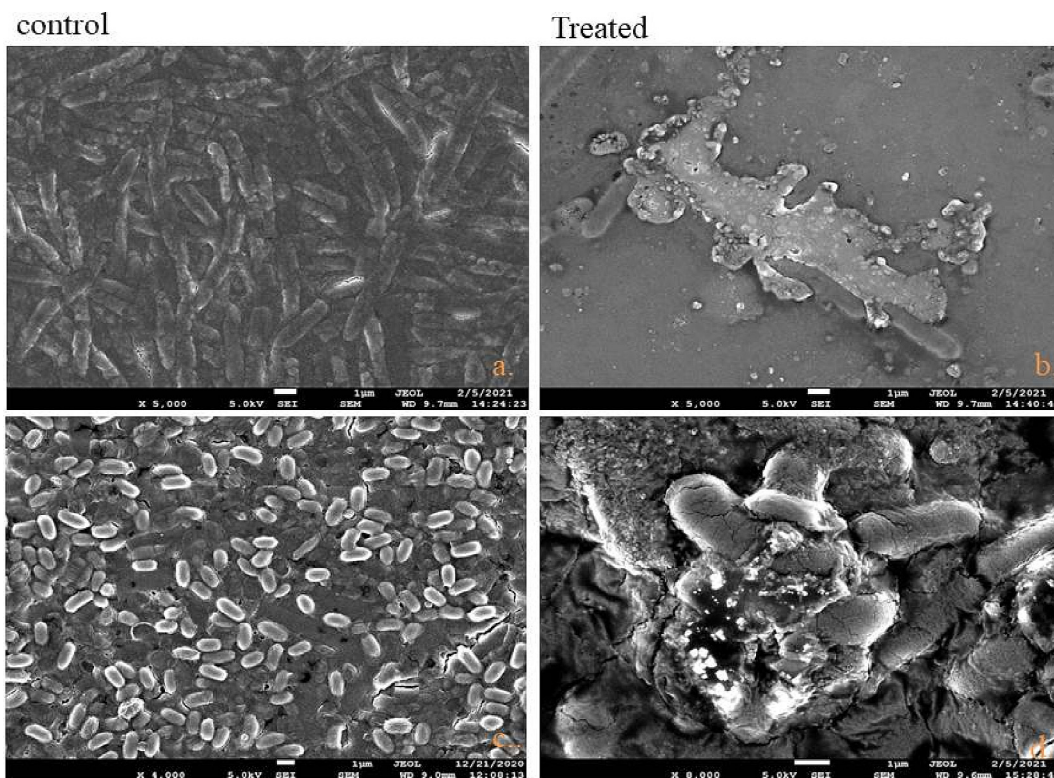


Fig. 8. FE-SEM images of bacteria treated with *Nyc*-AgNPs: (a,b) control & *Nyc*-AgNPs treated *E. coli* (c,d) control & *Nyc*-AgNPs treated *S. aureus*. Control without any treatment demonstrates integrated, while treated bacteria show rumples & disintegration in cell membranes.

ment. *S. aureus* & *E. coli* bacterial strains without NPs treatment considered as control showed smooth and damage free cells. While, *Nyc*-AgNPs treated *E. coli* and *S. aureus* showed intense changes in their cell surface morphology. In the treated cells, major changes were found in the membrane of bacterial cells

i.e. membrane integrity was completely lost and rumples was also observed (Fig. 8). The membrane integrity loss and formation of rumples in the treated bacterial cells were analogous with some previous findings (Anwar et al., 2019; Krishna et al., 2015).

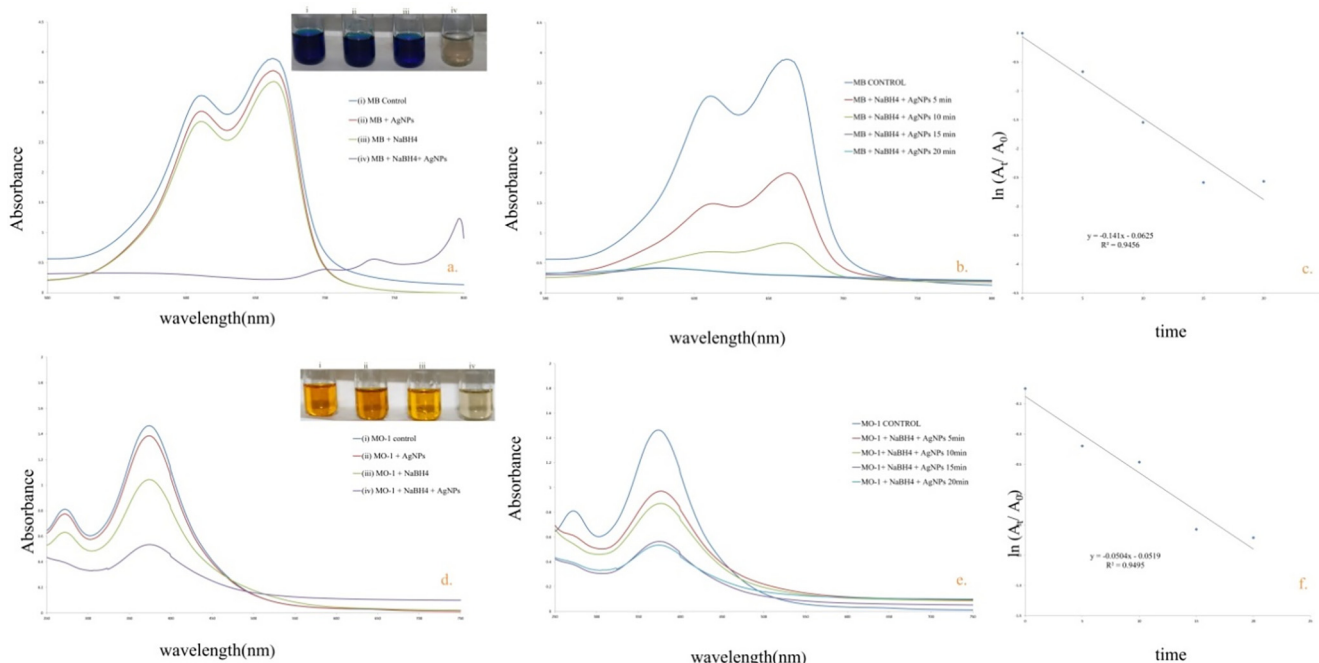


Fig. 9. a,b) UV-Vis spectra of NaBH_4 & *Nyc*-AgNPs mediated degradation of MB c; d,e) UV-Vis spectra of NaBH_4 & *Nyc*-AgNPs mediated degradation of MO-1c,f) Pseudo first order kinetic plot for the degradation of MB & MO-1-respectively.

3.10. Catalytic degradation of dyes

UV–vis spectrum of MB and MO-1 showed distinct peaks at 665 and 385 nm respectively (Edison et al., 2020). In the control reaction, solely NaBH₄ and AgNPs did not show degradation of the studied dyes (Fig. 9 a,d). Furthermore, after addition of AgNPs in the reaction mixture, containing MB/MO-1 with NaBH₄, efficient catalytic degradation was observed. Fig. 9b,e clearly depicted the absorbance intensity of MO-1 & MB i.e. steadily dropped with the addition of NaBH₄ + *Nyc.*-AgNPs as the reaction time passes, signifying that *Nyc.*-AgNPs have substantial catalytic efficiency. To predict the degradation efficiency of AgNPs + NaBH₄ in pseudo-first-order, Pseudo-first-order kinetic plot was also represented Fig. 9c,e. Moreover, degradation process of MB & MO-1 and response time were revealed in the form of linear correlation. The rate constant was calculated using Eq. (2) and is found 0.141 & 0.050 min⁻¹ for MB & MO-1 respectively. Formerly, adjacent values of rate constant (k) for the degradation of methylene blue has also been reported (Edison et al., 2020; Somasundaram et al., 2021). Moreover, the MB & MO-1 degrading efficacy was deliberate to be >80%. Therefore, the green synthesized AgNPs from NAT substantiated to be a potential & reliable catalyst to degrade MB.

4. Conclusion

N. arbor-tristis mediated silver NPs were synthesised using safer, rapid & eco-friendly green approach. The biogenic Ag nanoparticles were formed via reduction of silver (Ag⁺) ions using NAT fruit extract. The phytosynthesized *Nyc.*-AgNPs were spherical with an average size of 20–60 nm. In addition, these synthesised AgNPs showed efficient ability to reduce infection causing bacteria & fungi, which highlights the therapeutic value of these particles as antimicrobial agent against different bacterial & fungal strains such as *S. aureus*, *E. coli*, *P. fragi*, *P. syringae*, *S. epidermidis* and *A. flavus*. This is first report on *Nyctanthes* fruit-based biocompatible & bio-fabricated AgNPs. These cytotoxic effects of synthesized AgNPs will provide an opportunity to the pharmaceutical companies to design drugs using the biogenic NPs against the disease caused by the test organisms. Besides, *Nyc.*-AgNPs can be recommended as an efficient nanocatalyst for eliminating pollutants. Moreover, along with efficient degradation potential, for industrial scale technology, it is also important to study the proper integration of catalyst with conventional technologies, its stability and its recyclability for long term sustainability in actual field conditions

Ethics approval

N/A.

Consent to participate

All authors consent to participate in this manuscript.

Consent for publication

All authors consent to publish this manuscript in Journal of King Saud University-Science.

Availability of data and material

Data will be available on request to corresponding or first author.

Code availability

Not Applicable.

Declaration of Competing Interest

The authors declare that they have no known competing financial interests or personal relationships that could have appeared to influence the work reported in this paper.

Acknowledgments

Authors are gratified to CAIF (Central Analytical facilities) and SAIF (Sophisticated Analytical Instrument Facility) at MUJ for providing facilities to perform different type of characterization techniques including Uv-visible spectroscopy, EDX, XRD, FTIR, SEM & TGA & also thankful to MNIT Jaipur for TEM & zeta potential analysis.

References

- Abdulsahib, S.S., 2021. Synthesis, characterization and biomedical applications of silver nanoparticles. *Biomed.* <https://doi.org/10.51248/v41i2.1058>.
- Adnan, M., Akbar, A., Mussarat, S., Murad, W., Hameed, I., Begum, S., Nazir, R., Ali, N., Ali, E.A., Bari, A., 2022. Phyto-extract-mediated synthesis of silver nanoparticles (AgNPs) and their biological activities. *Biomed. Res. Int.* 2022.
- Ali, K., Ahmed, B., Dwivedi, S., Saquib, Q., Al-Khedhairi, A.A., Musarrat, J., 2015. Microwave accelerated green synthesis of stable silver nanoparticles with Eucalyptus globulus leaf extract and their antibacterial and antibiofilm activity on clinical isolates. *PLoS One.* <https://doi.org/10.1371/journal.pone.0131178>.
- Ali, M., Kim, B., Belfield, K.D., Norman, D., Brennan, M., Ali, G.S., 2016. Green synthesis and characterization of silver nanoparticles using Artemisia absinthium aqueous extract - A comprehensive study. *Mater. Sci. Eng. C.* <https://doi.org/10.1016/j.msec.2015.08.045>.
- Al-Rajhi, A.M.H., Salem, S.S., Alharbi, A.A., Abdelghany, T.M., 2022. Ecofriendly synthesis of silver nanoparticles using Kei-apple (*Dovyalis caffra*) fruit and their efficacy against cancer cells and clinical pathogenic microorganisms. *Arab. J. Chem.* 15, 103927.
- Anwar, A., Masri, A., Rao, K., Rajendran, K., Khan, N.A., Shah, M.R., Siddiqui, R., 2019. Antimicrobial activities of green synthesized gums-stabilized nanoparticles loaded with flavonoids. *Sci. Rep.* <https://doi.org/10.1038/s41598-019-39528-0>.
- Ashour, A.A., Raafat, D., El-Gowell, H.M., El-Kamel, A.H., 2015. Green synthesis of silver nanoparticles using cranberry powder aqueous extract: Characterization and antimicrobial properties. *Int. J. Nanomedicine.* <https://doi.org/10.2147/IJN.587268>.
- Atalar, M.N., Baran, A., Baran, M.F., Keskin, C., Aktepe, N., Yavuz, Ö., İrtügen Kandemir, S., 2021. Economic fast synthesis of olive leaf extract and silver nanoparticles and biomedical applications. *Part. Sci. Technol.* <https://doi.org/10.1080/02726351.2021.1977443>.
- Balachandar, R., Navaneethan, R., Biruntha, M., Kumar, K.K.A., Govarthanan, M., Karmegam, N., 2022. Antibacterial activity of silver nanoparticles phytosynthesized from *Glochidion candolleianum* leaves. *Mater. Lett.* 311, 131572.
- Bogireddy, N.K.R., Kumar, H.A.K., Mandal, B.K., 2016. Biofabricated silver nanoparticles as green catalyst in the degradation of different textile dyes. *J. Environ. Chem. Eng.* 4, 56–64.
- Castillo-Henríquez, L., Alfaro-Aguilar, K., Ugalde-Álvarez, J., Vega-Fernández, L., Montes de Oca-Vásquez, G., Vega-Baudrit, J.R., 2020. Green synthesis of gold and silver nanoparticles from plant extracts and their possible applications as antimicrobial agents in the agricultural area. *Nanomaterials* 10, 1763.
- Cheng, K.M., Hung, Y.W., Chen, C.C., Liu, C.C., Young, J.J., 2014. Green synthesis of chondroitin sulfate-capped silver nanoparticles: Characterization and surface modification. *Carbohydr. Polym.* <https://doi.org/10.1016/j.carbpol.2014.03.053>.
- Coates, J., 2006. Interpretation of Infrared Spectra, A Practical Approach. In: *Encyclopedia of Analytical Chemistry.* <https://doi.org/10.1002/9780470027318.a5606>.
- David, L., Moldovan, B., 2020. Green synthesis of biogenic silver nanoparticles for efficient catalytic removal of harmful organic dyes. *Nanomaterials.* <https://doi.org/10.3390/nano10020202>.
- de Jesús Ruiz-Baltazar, Á., Reyes-López, S.Y., Larrañaga, D., Estévez, M., Pérez, R., 2017. Green synthesis of silver nanoparticles using a *Melissa officinalis* leaf extract with antibacterial properties. *Results Phys.* 7, 2639–2643.
- Dhiman, M., Sharma, L., Singh, A., Sharma, M.M., 2021. Biogenic fabrication of silver nanoparticles using *Sterculia urens* Roxb. And assessment of their antimicrobial efficiency. *Mater. Today Proc.* <https://doi.org/10.1016/j.matpr.2021.01.732>.
- Edison, T.N.J.I., Atchudan, R., Karthik, N., Balaji, J., Xiong, D., Lee, Y.R., 2020. Catalytic degradation of organic dyes using green synthesized N-doped carbon supported silver nanoparticles. *Fuel.* <https://doi.org/10.1016/j.fuel.2020.118682>.

- Faisal, S., Shah, S.A., Shah, S., Akbar, M.T., Jan, F., Haq, I., Baber, M.E., Aman, K., Zahir, F., Bibi, F., Syed, F., Iqbal, M., Jawad, S.M., Salman, S., 2020. In vitro biomedical and photo-catalytic application of bio-inspired zingiber officinale mediated silver nanoparticles. *J. Biomed. Nanotechnol.* <https://doi.org/10.1166/jbn.2020.2918>.
- Fito, J., Abrahm, S., Angassa, K., 2020. Adsorption of Methylene Blue from Textile Industrial Wastewater onto Activated Carbon of Parthenium hysterophorus. *Int. J. Environ. Res.* <https://doi.org/10.1007/s41742-020-00273-2>.
- Ghotekar, S., Pansambal, S., Pawar, S.P., Pagar, T., Oza, R., Bangale, S., 2019. Biological activities of biogenically synthesized fluorescent silver nanoparticles using *Acanthospermum hispidum* leaves extract. *SN Appl. Sci.* 1, 1–12.
- Gou, Y., Zhou, R., Ye, X., Gao, S., Li, X., 2015. Highly efficient in vitro biosynthesis of silver nanoparticles using *Lysinibacillus sphaericus* MR-1 and their characterization. *Sci. Technol. Adv. Mater.* <https://doi.org/10.1088/1468-6996/16/1/015004>.
- Guerra, J.D., Sandoval, G., Patron, A., Avalos-Borja, M., Pstryakov, A., Garibo, D., Susarrey-Arce, A., Bogdanchikova, N., 2020. Selective antifungal activity of silver nanoparticles: A comparative study between *Candida tropicalis* and *Saccharomyces boulardii*. *Colloids Interface Sci. Commun.* <https://doi.org/10.1016/j.colcom.2020.100280>.
- Gul, A., Shaheen, A., Ahmad, I., Khattak, B., Ahmad, M., Ullah, R., Bari, A., Ali, S.S., Alobaid, A., Asmari, M.M., 2021. Green synthesis, characterization, enzyme inhibition, antimicrobial potential, and cytotoxic activity of plant mediated silver nanoparticle using *Ricinus communis* leaf and root extracts. *Biomolecules* 11, 206.
- Gupta, A., Mumtaz, S., Li, C.-H., Hussain, I., Rotello, V.M., 2019. Combatting antibiotic-resistant bacteria using nanomaterials. *Chem. Soc. Rev.* 48, 415–427.
- Haggag, E.G., Elshamy, A.M., Rabeh, M.A., Gabr, N.M., Salem, M., Youssif, K.A., Samir, A., Bin Muhsinah, A., Alsayari, A., Abdelmohsen, U.R., 2019. Antiviral potential of green synthesized silver nanoparticles of *lampranthus coccineus* and *malephora lutea*. *Int. J. Nanomedicine.* <https://doi.org/10.2147/IJN.S214171>.
- Hamouda, R.A., Hussein, M.H., Abo-elmagd, R.A., Bawazir, S.S., 2019. Synthesis and biological characterization of silver nanoparticles derived from the cyanobacterium *Oscillatoria limnetica*. *Sci. Rep.* <https://doi.org/10.1038/s41598-019-49444-y>.
- Holzwarth, U., Gibson, N., 2011. The Scherrer equation versus the “Debye-Scherrer equation”. *Nat. Nanotechnol.* <https://doi.org/10.1038/nnano.2011.145>.
- Jain, N., Jain, P., Rajput, D., Patil, U.K., 2021. Green synthesized plant-based silver nanoparticles: Therapeutic prospective for anticancer and antiviral activity. *Micro Nano Syst. Lett.* 9, 1–24.
- Jebiril, S., Khanfir Ben Jenana, R., Dridi, C., 2020. Green synthesis of silver nanoparticles using *Melia azedarach* leaf extract and their antifungal activities: In vitro and in vivo. *Mater. Chem. Phys.* <https://doi.org/10.1016/j.matchemphys.2020.122898>.
- Jusoh, R., Kamarudin, N.H.N., Kamarudin, N.S., Sukor, N.F., 2019. Green synthesis of spherical shaped silver nanoparticles using allium cepa leaves extract and its photocatalytic activity. in: *Materials Science Forum.* <https://doi.org/10.4028/www.scientific.net/MSF.962.57>.
- Kedi, P.B.E., Meva, F.E., Kotsedi, L., Nguemfo, E.L., Zangueu, C.B., Ntomba, A.A., Mohamed, H.E.A., Dongmo, A.B., Maaza, M., 2018. Eco-friendly synthesis, characterization, in vitro and in vivo anti-inflammatory activity of silver nanoparticle-mediated *Selaginella myosurus* aqueous extract. *Int. J. Nanomedicine.* <https://doi.org/10.2147/IJN.S174530>.
- Khane, Y., Benouis, K., Albukhaty, S., Sulaiman, G.M., Abomughaid, M.M., Al Ali, A., Aouf, D., Fenniche, F., Khane, S., Chaibi, W., 2022. Green synthesis of silver nanoparticles using aqueous Citrus limon zest extract: Characterization and evaluation of their antioxidant and antimicrobial properties. *Nanomaterials* 12, 2013.
- Kredy, H.M., 2018. The effect of pH, temperature on the green synthesis and biochemical activities of silver nanoparticles from *Lawsonia inermis* extract. *J. Pharm. Sci. Res.*
- Krishna, G., Kumar, S.S., Pranitha, V., Alha, M., Charaya, S., 2015. Biogenic synthesis of silver nanoparticles and their synergistic effect with antibiotics: A study against *Salmonella* SP. *Int. J. Pharm. Pharm. Sci.*
- Kumar, R., Ghoshal, G., Jain, A., Goyal, M., 2017. Rapid green synthesis of silver nanoparticles (AgNPs) using (*Prunus persica*) plants extract: exploring its antimicrobial and catalytic activities. *J. Nanomed. Nanotechnol.* 8, 1–8.
- Kumar, V., Singh, S., Srivastava, B., Bhadouria, R., Singh, R., 2019. Green synthesis of silver nanoparticles using leaf extract of *Holoptelea integrifolia* and preliminary investigation of its antioxidant, anti-inflammatory, antidiabetic and antibacterial activities. *J. Environ. Chem. Eng.* <https://doi.org/10.1016/j.jece.2019.103094>.
- Mittal, J., Singh, A., Batra, A., Sharma, M.M., 2017. Synthesis and characterization of silver nanoparticles and their antimicrobial efficacy. *Part. Sci. Technol.* 35, 338–345. <https://doi.org/10.1080/02726351.2016.1158757>.
- Mittal, J., Pal, U., Sharma, L., Verma, A.K., Ghosh, M., Sharma, M.M., 2020. Unveiling the cytotoxicity of phytosynthesized silver nanoparticles using *Tinospora cordifolia* leaves against human lung adenocarcinoma A549 cell line. *IET Nanobiotechnol.* <https://doi.org/10.1049/iet-nbt.2019.0335>.
- Moodley, J.S., Krishna, S.B.N., Pillay, K., Sershen, Govender, P., 2018. Green synthesis of silver nanoparticles from *Moringa oleifera* leaf extracts and its antimicrobial potential. *Adv. Nat. Sci. Nanosci. Nanotechnol.* <https://doi.org/10.1088/2043-6254/aaabb2>.
- Ojha, S., Sett, A., Bora, U., 2017. Green synthesis of silver nanoparticles by *Ricinus communis* var. *carmencita* leaf extract and its antibacterial study. *Adv. Nat. Sci. Nanosci. Nanotechnol.* 8, 35009.
- Oves, M., Rauf, M.A., Aslam, M., Qari, H.A., Sonbol, H., Ahmad, I., Zaman, G.S., Saeed, M., 2022. Green synthesis of silver nanoparticles by *Conocarpus Lancifolius* plant extract and their antimicrobial and anticancer activities. *Saudi J. Biol. Sci.* 29, 460–471.
- Pandey, S., Do, J.Y., Kim, J., Kang, M., 2020. Fast and highly efficient catalytic degradation of dyes using κ -carrageenan stabilized silver nanoparticles nanocatalyst. *Carbohydr. Polym.* <https://doi.org/10.1016/j.carbpol.2019.115597>.
- Samanta, S., Banerjee, J., Das, B., Mandal, J., Chatterjee, S., Ali, K.M., Sinha, S., Giri, B., Ghosh, T., Dash, S.K., 2022. Antibacterial potency of cyto-compatible chitosan-decorated biogenic silver nanoparticles and molecular insights towards cell-particle interaction. *Int. J. Biol. Macromol.* 219, 919–939.
- Seifipour, R., Nozari, M., Pishkar, L., 2020. Green synthesis of silver nanoparticles using *Tragopogon collinus* leaf extract and study of their antibacterial effects. *J. Inorg. Organomet. Polym. Mater.* 30, 2926–2936.
- Sharifi-Rad, M., Pohl, P., Epifano, F., 2021. Phytofabrication of silver nanoparticles (AgNPs) with pharmaceutical capabilities using *Otostegia persica* (burm.) Boiss. leaf extract. *Nanomaterials* 11, 1045.
- Somasundaram, C.K., Atchudan, R., Edison, T.N.J.L., Perumal, S., Vinodh, R., Sundramoorthy, A.K., Babu, R.S., Alagan, M., Lee, Y.R., 2021. Sustainable synthesis of silver nanoparticles using marine algae for catalytic degradation of methylene blue. *Catalysts.* <https://doi.org/10.3390/catal11111377>.
- Sukumar, D.T., Gunasankaran, G., Arumugam, V.A., Muthukrishnan, S., 2022. Effects of biogenic synthesis of chitosan entrapped silver nanoparticle from *Aegle marmelos* on human cervical cancer cells (HeLa). *J. Drug Deliv. Sci. Technol.* <https://doi.org/10.1016/j.jddst.2022.103189>.
- Thiruvengadam, V., Bansod, A.V., 2020. Characterization of silver nanoparticles synthesized using chemical method and its antibacterial property. *Biointerface Res. Appl. Chem.* <https://doi.org/10.33263/BRIAC106.72577264>.
- Traiwatcharanon, P., Timsorn, K., Wongchoosuk, C., 2017. Flexible room-temperature resistive humidity sensor based on silver nanoparticles. *Mater. Res. Express.* <https://doi.org/10.1088/2053-1591/aa85b6>.
- Tripathi, D.K., Shweta, Singh, Shweta, Singh, Swati, Pandey, R., Singh, V.P., Sharma, N.C., Prasad, S.M., Dubey, N.K., Chauhan, D.K., 2017. An overview on manufactured nanoparticles in plants: Uptake, translocation, accumulation and phytotoxicity. *Plant Physiol. Biochem.* <https://doi.org/10.1016/j.plaphy.2016.07.030>.
- Tyavambaza, C., Elbagory, A.M., Madiehe, A.M., Meyer, M., Meyer, S., 2021. The antimicrobial and anti-inflammatory effects of silver nanoparticles synthesized from *Cotyledon orbiculata* aqueous extract. *Nanomaterials.* <https://doi.org/10.3390/nano11051343>.
- Varadavenkatesan, T., Selvaraj, R., Vinayagam, R., 2019. Dye degradation and antibacterial activity of green synthesized silver nanoparticles using *Ipomoea digitata* Linn. flower extract. *Int. J. Environ. Sci. Technol.* <https://doi.org/10.1007/s13762-018-1850-4>.
- Verma, A., Mehata, M.S., 2016. Controllable synthesis of silver nanoparticles using *Neem* leaves and their antimicrobial activity. *J. Radiat. Res. Appl. Sci.* <https://doi.org/10.1016/j.jrras.2015.11.001>.